Biomedical Signal Processing and Control 87 (2024) 105409

Contents lists available at ScienceDirect

Biomedical Signal Processing and Control

journal homepage: www.elsevier.com/locate/bspc

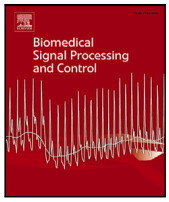

Prediction of therapy for ischemic heart disease from PPG signals using fuzzy GRU network

Poulomi Pal, Manjunatha Mahadevappa *

School of Medical Science and Technology, Indian Institute of Technology Kharagpur, India

ARTICLE INFO

Keywords:
Ischemic heart disease
Gated recurrent unit
Fuzzy logic
Choquet integral
Recurrent network

ABSTRACT

Background Cardiac morbidity like ischemic heart disease (IHD) causes global mortality. Diagnosis of IHD requires coronary angiograms — an invasive, sophisticated, and expensive procedure. However, non-invasive methods could not gain much confidence in swift diagnosis of IHD patients. These potential issues provided the research motivation for diagnosing IHD priorly in this pilot study.

Objective A computer-aided technique, as an alternate method to fasten and ease IHD detection and categorization, has been suggested in this cohort study. Here, the classification was conducted by a sandwich model of GRU and fuzzy logic in a deep GRU Fuzzy network.

Methods In this work, photoplethysmography (PPG) signals were acquired from 355 IHD patients. Gabor–Winger transform was used to derive signal features using statistical identities. Analysis was done with a Fuzzy GRU Network comprising GRU and BiGRU layers with fuzzy layers. An algorithm was designed with a Rete network and three membership functions to deduce fuzzy inference. Then, Choquet Integral was used for defuzzification.

Results The proposed network predicted results with 0.85 accuracy, 0.86 recall, 0.84 precision, 0.86 sensitivity, 0.78 Micro-averaged F1-score, and 0.84 specificity. The network architecture was validated using ablation and comparative studies. The PRC and ROC curves gave the highest values of 0.91 AP and 0.90 AUC, respectively for this network. A state-of-the-art study was done to show the superiority of the technique.

Conclusion This computer-aided model using PPG might become a tool in predicting the type of therapy for IHD patients which will provide a non-invasive, inexpensive, and fast mode of diagnosis.

1. Introduction

One of the common cardiovascular diseases (CVD) which affects people globally is ischemic heart disease (IHD). As per the database of the Global Burden of Disease Study 2017, 126.5 million patients suffered from IHD [1]. It is expected to increase from 1655 to 1845 per 100,000 population size, by a decade [2]. IHD occurs when there is a deprivation in the supply and demand of myocardial oxygen leading to hypoxia [3]. This happens due to atherosclerosis, an obstruction (lesion) of blood flow that occurs inside the coronary arteries, creating a blockage (stenosis) [3]. Thus, the performance of the heart (pumping activity) decreases as well as the circulation of blood throughout the body.

Clinicians diagnose IHD by ECG, echocardiogram, coronary artery angiography (CAG), and intravascular ultrasound [4]. For critical IHD patients, CAG is indispensable because it confirms whether the patient has normal coronary arteries or lesions can be cured by medicines or stenosis has been affected such, that patient needs to undergo surgery. Being invasive, CAG depends on injecting radio-opaque dyes, which possess side effects on kidneys [5,6]. This increases the risk further under co-morbid cases [7]. The challenge arises when the right balance is required between the safety, accuracy, and convenience of the patients. Thus, there is a need to find an alternative to such invasive methods which has the risk of radiation exposure. Moreover, the detection techniques should be affordable for developing and under-developed countries.

IHD detection has been done using non-invasive techniques-impedance cardiography (ICG), photoplethysmography (PPG), phonocardiography (PCG), etc. In this regard, the PPG signal carries information on cardiac pumping activity which has become very resourceful among biomedical experts [8]. Several works employing PPG signals have been carried out with different methods for detecting IHD [9,10]. For example, machine learning techniques were used to detect IHD patients using time domain analysis of PPG signals [11]. Banerjee et al. identified patients using SVM on the MIMIC II dataset and hospital

* Corresponding author.
E-mail address: mmaha2@smst.iitkgp.ac.in (M. Mahadevappa).

https://doi.org/10.1016/j.bspc.2023.105409
Received 8 July 2023; Received in revised form 26 August 2023; Accepted 11 September 2023
Available online 27 September 2023

Table 1
Patient details obtained clinically.

	No Treatment (T)	Medication (M)	Surgery (S)
He/She (118)	80/38	85/33	88/30
Age	48.15 ± 10.47	58.11 ± 9.87	57.64 ± 11.29
Height (cm)	163.71 ± 4.10	164.34 ± 5.28	167.22 ± 7.91
Weight (kg)	59.82 ± 9.43	62.75 ± 11.47	61.75 ± 10.85
BMI	22.20 ± 7.31	23.10 ± 8.05	21.90 ± 9.64
Heart rate (pulse)	79.21 ± 5.74	78.03 ± 12.33	77.93 ± 9.78
SBP (mm-of-Hg)	81.72 ± 10.50	82.11 ± 11.02	80.54 ± 9.86
DBP (mm-of-Hg)	119.13 ± 6.94	121.06 ± 18.70	123.24 ± 15.97
Smoking	5%	33%	27%
Hypertension	40%	69%	71%
Diabetes	3%	4%	2%
Dislipidemia	31%	38%	41%

data yielding specificity and sensitivity of 0.80 [12]. Hosseini et al. used PPG and ECG signals to distinguish between various degrees of stenosis in coronary arteries on clinical data of 48 patients [13]. Fathieh et al. classified 408 CAD patients applying Elastic Net model producing AUC of 0.90 [14]. In another work, pulse wave information of PPG in spectral-domain was utilized to assess the 193 IHD patients with specificity of 0.70 and sensitivity of 0.83 [15]. Coupling of PPG signal with PCG could classify IHD patients with 80% accuracy [16]. However, these methods were limited by the cohort size and result-like accuracy, sensitivity, specificity, etc. Later, Antonio et al. have studied the neuro-fuzzy systems in medical applications [17]. Artificial neural network (ANN) with fuzzy inference has been utilized to diagnose IHD in its chronic stable form with an accuracy of 82% by Silveri et al. [18]. However, no non-invasive studies were done to categorize the stages of IHD patients based on their coronary artery condition.

In this work, we attempted to improve the existing PPG-based study by introducing fuzzy logic concepts inside a gated recurrent unit (GRU) network for the classification of IHD patients based on the therapy suggested by cardiologists. If the coronary arteries of patients were normal during CAG, they were categorized into a group of subjects requiring no treatment (T). On observing minor blocks in the vessels, medicines prescribed were for healing the patients' arteries (M). When the patient had stenosis in more than two arteries and the lesions blocked the vessels by >90%, in those cases either PCI or CABG was opted for (S). For categorizing such groups a novel Deep GRU Fuzzy Network (DGFN) has been proposed here. The fuzzy membership properties along with the idea of the Rete algorithm were implemented for fuzzification. Concept of Choquet integral as an aggregating method was used in defuzzification. The input database for DGFN execution was created by acquiring data in the hospital.

2. Materials and methods

2.1. Data collection

Collection of PPG signals was conducted from patients visiting the Cardiology Unit of Medical College and Hospital in Kolkata, India. Institutional Ethical Clearance was attained for this study. Inclusion and exclusion criteria were followed and informed consent was obtained from cohorts. The demographic details of all the subjects in the three groups are displayed in Table 1. The instrumental setup for PPG signal collection included the IR Plethysmograph Velcro Strap (MLT 1020 PPG) as the PPG sensor and a data acquisition device (DAQ) — Power Lab 8/35 (ML135) both from AD Instruments, Sydney (Australia of 16-bit resolution). The CAG reports from cardiologists were the *gold standard* information. Fig. 1 shows the CAG reports of IHD patients having lesions in their coronary arteries.

Table 2
Statistical features obtained from the distribution values.

	Quantity	Equation
1	Maximum	$max(d_i)$
2	Minimum	$min(d_i)$
3	Mean	$\frac{\sum(d_i)}{n}$
4	Median	$\frac{d_{n/2}+d_{n/2+1}}{2}$ or $\frac{d_{(n+1)/2}}{2}$
5	Mode	d_i which occurs most frequently
6	Variance	$\frac{\sum(d_i-Mean)^2}{n}$
7	Standard Deviation	$\sqrt{\frac{\sum(d_i-Mean)^2}{n}}$
8	Entropy	$-\sum(p.*log2(p))$, where p = histogram of d
9	Power	$\frac{\sum(d_i)^2}{2n}$
10	Energy	$\sum(d_i)^2$
11	Skewness	$3*\frac{(Mean-Median)}{Standard\ Deviation}$
12	Kurtosis	$n*\frac{\sum(d_i-Mean)^4}{\sum(d_i-Mean^2)^2}$
13	Root Mean Square	$\sqrt{\frac{\sum(d_i)^2}{n}}$
14	Coefficient of Variance	$\frac{Standard\ Deviation}{Mean}$
15	Interquartile range	$Median(d_{n/2}....d_n)-Median(d_1....d_{n/2})$

2.2. Network input

Each PPG signal was collected for 120 s. This experimental study was conducted with signals comprising 1,00,000 data points. All the signals were filtered using a bandpass Butterworth filter (order 8) with 0.2–12 Hz as the cut-off frequency and a 50 Hz notch filter. Baseline correction was also performed. The total number of PPG signals collected from patients was 355. Among them, one patient's data was removed due to low SNR compared to other signals. For this study, 354 patients were grouped into three divisions: T = 118, M = 118, and S = 118. They were grouped into testing and training data in the ratio of 15:85 and validation data was 20% of training data. Since data was low in number signal augmentation was performed using left and right shifting, compression and expansion, and speeding up and speeding down techniques on 240 signals for training. Now, 1440 signals were used in training. Raw signals were intact for validation and testing. Augmentation was done only for training data to prevent data leakage.

A window comprising 10,000 data points was moved across the entire length of each signal with a gap of 10 points. Each window segment (x) was converted to the time–frequency (tf) domain from the time domain using Gabor–Wigner transformation (GWT) [19] for extracting signal features (shown in Fig. 2). In a tf distribution, a high resolution was obtained in both domains, which made analysis and interpretation easier by reducing the computational complexity. Statistical analysis was performed over the distribution values d from the $GWT_x(t,f)$ of x to extract relevant quantitative information as listed in Table 2 and shown in Fig. 2. Each x gave 15 statistical features resulting in 15 × 90 features/signal.

2.3. Network architecture

The proposed network architecture of DGFN is illustrated in Fig. 3. It comprised an input layer with signal features (450 × 1 dimension), GRU layers, BiGRU layers, feedforward(FF) layers, and multi-layer perceptron (MLP). A fuzzy layer was introduced in between fully connected layer 1 (FCL1) and fully connected layer 2 (FCL2). The network ended with a softmax layer and a classification layer.

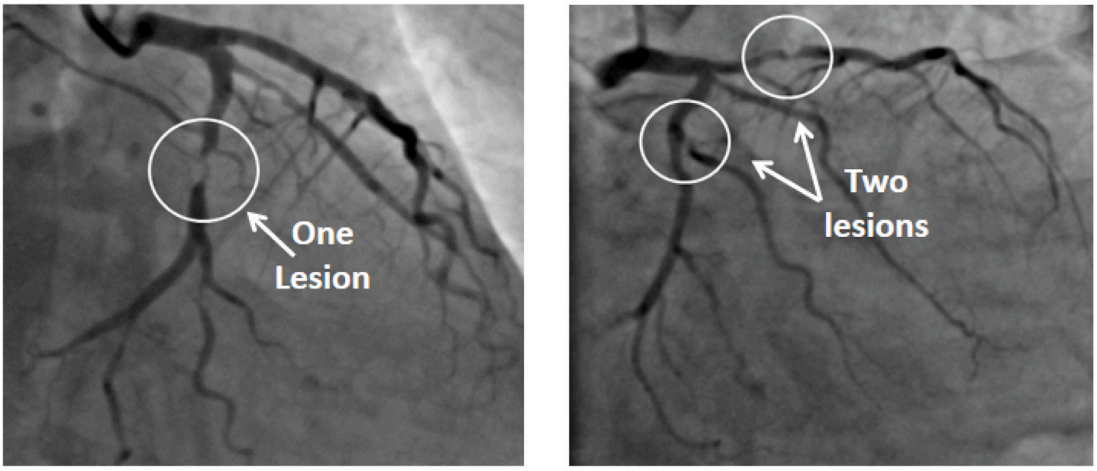

(a) (b)

Fig. 1. (a) CAG diagram showing one artery block and (b) CAG diagram showing two artery blocks.

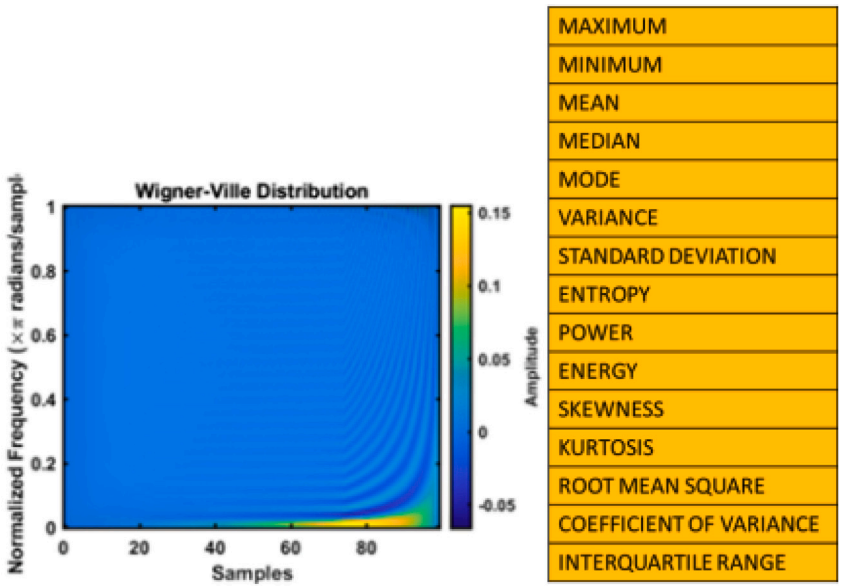

Fig. 2. The Gabor–Wigner transformation and vector of input features extracted from the distribution values by statistical analysis which will be given to the network input layer.

2.3.1. Deep GRU section

GRU (introduced by Cho et al. [20]) comprises an update gate and a reset gate but does not have an output gate (avoiding second non-linearity). They use fewer training parameters, use less memory, and execute faster. Here, GRU layers have been used because of their advantage over LSTM and BiLSTM layers w.r.t. the speed of the network, and computational cost, when the results have to be obtained from fewer sequential data. In Fig. 3, the input layer was followed by a BiGRU layer (L1) (450 GRU cells in the forward and backward layer) and a GRU layer (L2) (500 GRU cells). One MLP comprising three hidden dense layers (L3, L4, and L5) was used. First, second, and third hidden layers of 500 tanh units, 500 sigmoid units, and 500 ReLU units, respectively. A GRU module extracted and stored feature values whereas the MLP module carried out the non-linear mapping of the input to output layers. Then successive layers of BiGRU layer (L6), FF layer (L7), GRU layer (L8), and FF layer (L9) were present. These layers formed a relationship between the input independent layers with the output dependent variables such that information flow was in the forward direction. In the end, adjacent layers of BiGRU and GRU were used. The values from the last GRU layer passed to the FCL1.

Algorithm 1 Steps executed in the fuzzy layer

Input: Crisp values resulting from the FCL1
Output: Fuzzified elements generated after the inference derivation

1: Forming a rete network for fuzzification
2: Rules are stored in working memory elements which gets triggered on meeting requisite condition
3: Pattern matching done on the basis of facts and conflict resolution in each node
4: Inference engine performs action using the alpha and beta memories following modus ponens
5: The fuzzified values are obtained after deduction action from the above step

2.3.2. Fuzzy layer

Sometimes, deep learning becomes too complex. To ease the computation, here we tried to incorporate fuzziness [21] inside a deep neural network. Fuzzy comes to the rescue when problems arise during

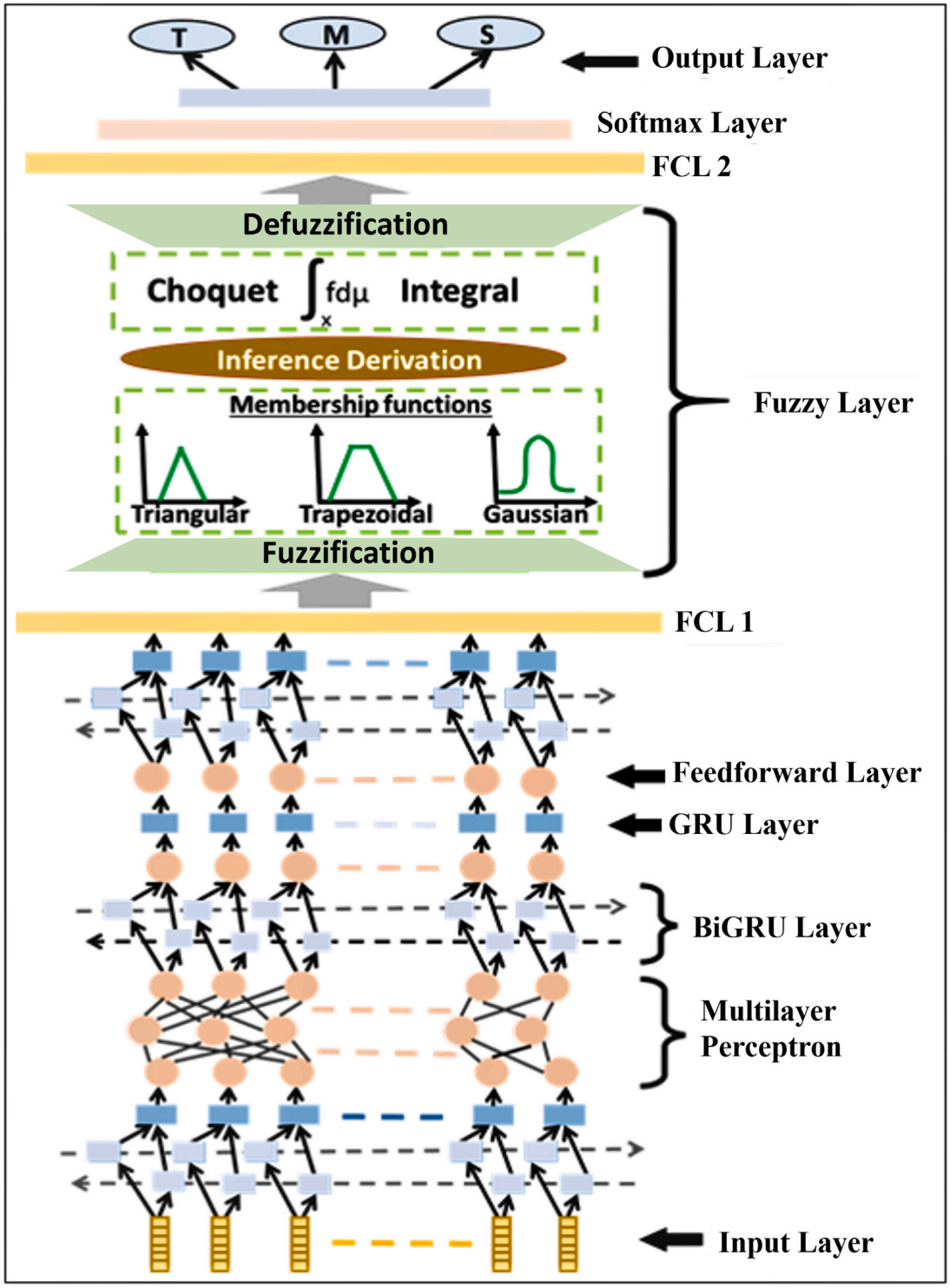

Fig. 3. Deep Gated Fuzzy Network (DGFN).

network execution i.e. when the weights in a neural network approach zero [22]. The concept of fuzzy inference introduces human-defined rule-based structures [23]. Thus, biased features can be generated and suitable feedback can be provided to the system [24]. Mechanism of fuzzy starts linear relations so, the non-linearity is handled by the fuzzy rules [25]. The introduction of fuzzy was done to alleviate complexity and make the system easy to understand and modify. It was seen that merging neural networks and fuzzy logic helps in overcoming respective drawbacks, leading to an increase in accuracy and a decrease in the time of training. The best part of fuzzy was that it helps in interpreting ambiguous data and deriving exact decisions [26].

In the proposed DGFN, the Fuzzy layer included three major steps — fuzzification, inference derivation, and defuzzification. The fuzzy rules (rule1, rule2, and rule3) were made up of fuzzy logic and its attributes. Thus crisp values (V_{crisp}) obtained from the FCL1 were converted to fuzzy values (V_{fuzzy}) by the process of fuzzification. The logic was built following the generalized modus ponens for fuzzy implications. This approach was similar to the concept of rule-based classifiers [27]. The

efficient and easy fuzzy inference was derived after studying the properties of the Rete network [28] using three different membership degrees. Here, Algorithm 1 was designed for implementing the fuzzy layer. Each node (N) in the Rete network performed the step of fuzzification. The selected threshold level as mentioned in (4), (6), and (8) is considered the pattern to be matched for obtaining the respective membership values. The working memory elements of the Rete network stored these threshold values. Initially, the pattern matching was followed by the individual and independent facts (fact1, fact2, and fact3) being sent to locations known as the alpha (α) memories. The facts were decided by observing the conditional statements and taking the conflict resolution into account. The combined facts after joining were stored in the locations known as the beta (β) memories. Now, alpha and beta memories were present inside the designated nodes of the Rete network. The decision-making was executed by the inference engine. This step was for inference derivation. Suitable conclusions we re-drawn by utilizing the alpha and beta memories inside the fuzzy layer. The final membership values (the fuzzified values) were generated using (5),(7), and (9) after the corresponding rules got satisfied, respectively.

It is already known that any membership function explains the way each input space point is connected or mapped to a particular membership value which is between 0 and 1. Now the choice of membership function depends on the manner of quantification to determine an input space as per the desired linguistic value meaning such as — big or small, high or low, positive or negative, etc. The other way it can be said that the selection of MF is proportional to the quantifying of the degree of truth. In this work, we wanted to quantify the feature values according to the statistical quantities (mean, and standard deviation) obtained after arranging the input in ascending order. Since the input values are not very chaotic the triangular and trapezoidal MFs were preferred. The triangular MF was used because it follows the technique of core-based reasoning i.e. decision-making is supported by experiences in the past. This MF solves problems by retrieving and re-implementing experience through adaptation. The trapezoidal MF can express the vagueness of information which is caused when linguistic assessments occur during the transformation into numeric variables. This MF follows core as well as support boundary (piecewise linear) based reasoning. For the above two MFs simplicity is the advantage. Whereas, Gaussian MF is known for smooth and concise notation. The Gaussian curve has the plus point of being non-zero and smooth at all input points.

All the feature values (the crisp values) of FCL1 were arranged in ascending order for carrying out the required statistical operations. The threshold values for the rules were decided using the variable $FeatureValue$ based on the average ($mean$) and standard deviation (std) of the entire set of FCL1 features.

If rule 1 was,

$$FeatureValue < mean - std \tag{1}$$

then fact 1 is a triangular membership function ($\mu_{triangle}$). The mathematical expression used was :

$$\mu_{triangle}(x; d, e, f) = max(min(\frac{x-d}{e-d}, \frac{f-x}{f-e}), 0) \tag{2}$$

where, the upper limit e is maximum value and lower limit d is minimum value among all the feature values.

If rule 2 was,

$$mean - std < FeatureValue < mean + std \tag{3}$$

then fact 2 is a Gaussian membership function ($\mu_{Gaussian}$). The mathematical expression used was :

$$\mu_{Gaussian}(x; c, \sigma) = e^{-\frac{1}{2}(\frac{x-c}{\sigma})^2} \tag{4}$$

where the c and σ represent center and width, respectively. Among the feature values of that layer, the median was used as c. The difference between the maximum and minimum values was used as σ.

Table 3
Details of layer architecture and parameters generated during the network execution.

Layers ascending from input till fuzzy	Activation functions	Hidden units/layers	Number of parameters
BiGRU	sigmoid	450	1645
GRU	tanh	500	1476
MLP	tanh, sigmoid, RELU	3	1825
BiGRU	sigmoid	450	1936
FF	RELU	1	3782
GRU	tanh	400	2589
FF	RELU	1	3264
BiGRU	sigmoid	450	4523
GRU	tanh	400	4136

Table 4
K-fold cross-validation result.

K-folds	Accuracy	Recall	Precision	Sensitivity	Specificity	MAF1-score
2	0.77	0.78	0.77	0.76	0.75	0.76
3	0.79	0.77	0.78	0.77	0.76	0.78
4	0.78	0.79	0.79	0.78	0.77	0.79
5	0.79	0.81	0.82	0.80	0.79	0.79
6	0.81	0.83	0.81	0.79	0.78	0.80
7	0.83	0.80	0.80	0.82	0.80	0.82
8	0.80	0.83	0.82	0.80	0.82	0.81
9	0.82	0.80	0.84	0.83	0.81	0.81
10	0.85	0.86	0.85	0.86	0.84	0.85
11	0.84	0.82	0.83	0.83	0.82	0.83
12	0.85	0.83	0.84	0.82	0.84	0.84
13	0.84	0.85	0.83	0.84	0.84	0.83

If rule 3 was,

$$FeatureValue > mean + std \tag{5}$$

then fact 3 is $\mu_{trapezoidal}$, a trapezoidal membership function. The mathematical expression used was:

$$\mu_{trapezoidal}(x; m, n, p, q) = \begin{cases} 0, & x \le m \\ \frac{x-m}{n-m}, & m < x \le n \\ 1, & n < x \le p \\ \frac{p-x}{q-p} & p < x \le q \\ 0, & \\ x \ge q & \end{cases} \tag{6}$$

where m is minimum value, n is minimum value + (median/2), p is maximum value −(median/2), and q was maximum value among all feature values.

Defuzzification was performed to convert the above generated V_{fuzzy} back to V_{crisp}. The Choquet Integral was used here as the defuzzification technique. This technique acted as the aggregation operator. Choquet integral provided an output variable that contains various importance along with the interactions among their generated values [29]. The feature values obtained from the Fuzzy layer were crisp so they were transferred to FCL2 for further analysis. The type 1 fuzzy controller was applied for tuning purposes whose performance was based on the backpropagation error values to control the fuzzy logic operation between FCL1 and FCL2 [30]. With each iteration, the controller efficiency enhanced the network performance. Detailed Pseudo code of DGFN has been given in Algorithms 2 and 3. Other parameters are elaborated on in the next section.

2.4. Hyper-parameter details

The stochastic gradient method-Adam optimizer was selected as a training algorithm for DGFN. The learning rate was decided after performing sensitivity analysis using a grid search over values ranging from 0.1 to 0.000001, where the best was 0.0001. The batch size was empirically derived as 30 on checking with 20–80 values. The

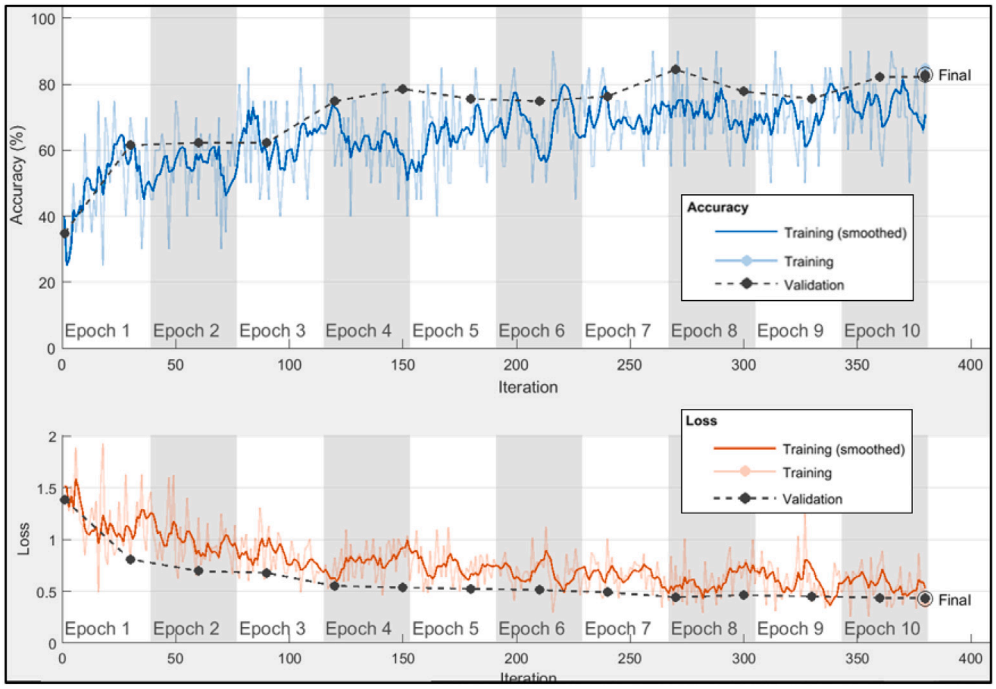

Fig. 4. Network performance graph showing change in accuracy and loss with respect to number of epochs and number of iterations during training and validation.

	T	S	M
T	528	39	46
S	40	325	55
M	38	51	279

Fig. 5. Confusion matrix.

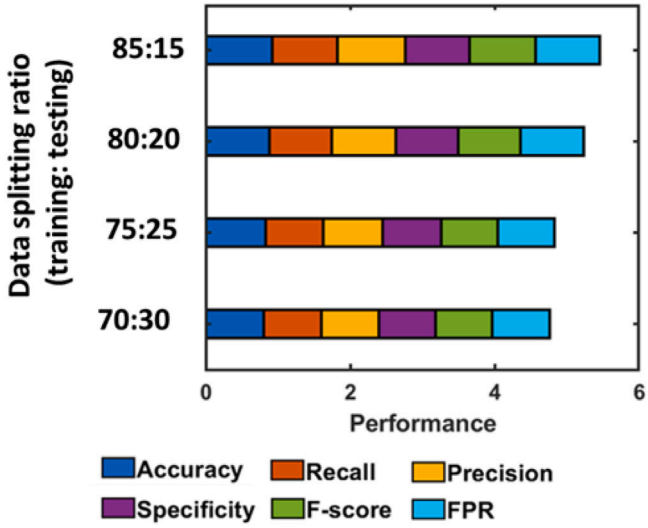

Fig. 6. Stack bar graph showing results of evaluation metrics after executing the network with different training: testing data splitting ratio.

epoch number was 15 after tuning manually with numerical figures 7–19. Shuffling was performed at the end of every epoch. Here, sparse categorical cross-entropy was used as the loss function. The momentum value was 0.9, the dropout was 0.2, and the square gradient decay factor was 0.99. Above mentioned hyperparameters were finalized after observing that the network was providing good accuracy without overfitting or underfitting. Experiments were carried out in ASUS TUF FX504 using MATLAB^{TM} (Mathworks INC.USA, R2020b).

3. Results

3.1. Performance evaluation

In order to classify IHD patients, the proposed network (DGFN) was trained and validated on collected data as per the performance curve shown in Fig. 4. With 15 epochs and 30 batches, the iterations conducted were 701. It was observed that there was no increment in the performance after 10 epochs or 375 iterations. Over-fitting occurs either due to the excess training of the model or the complexity of the deep neural network. Considering these two limitations, we standardized the network performance by batch normalization, regularization, cross-validation, and early stopping. Thus, based on the best value, final accuracy, and loss values were selected.

The training phase of DGFN was taken care of by the training algorithm — Adam optimizer. The fuzzy logic training was handled by the type 1 fuzzy controller. The RNN layers were executed as per the finalized hyperparameters such as the mini-batch size, momentum, epochs, etc. The iterative process during the training of DGFN was optimized using the weight parameters based on the back-propagated error with the motive to minimize loss. In the learning algorithm, the weights adjusted themselves. Here, the gradient descent algorithm and

Algorithm 2 Pseudo code for the designed model

Input: $x = [x_1, x_2, ..., x_{2130}]$, where $x_i = [1 \times 15]$ statistical features
for x in $x_{training}$, **do**
$L1 = \mathbf{GRU}_{forward}(x_i) \cdot \mathbf{GRU}_{backward}(x_i)$
(∵ BiGRU is forward pass & backward pass i.e. both directions)
$L2 = GRU_{forward}(L1)$
Multiple Layer Perceptron
$L3 = tanh(W_{MLP1}[L2] + b_{MLP1})$
$L4 = \sigma(W_{MLP2}[L3] + b_{MLP2})$
$L5 = ReLU(W_{MLP3}[L4] + b_{MLP3})$
$L1 = \mathbf{GRU}_{forward}(L3) \cdot \mathbf{GRU}_{backward}(L3)$
$L7 = ReLU(W_{feedforward}[L6] + b_{feedforward})$
$L8 = \mathbf{GRU}_{forward}(L7)$
$L9 = ReLU(W_{feedforward}[L8] + b_{feedforward})$
$L10 = \mathbf{GRU}_{forward}(L9) \cdot \mathbf{GRU}_{backward}(L9)$
$L11 = \mathbf{GRU}_{forward}(L10)$
Dropout Layer
$D = dropout(L11, d_{factor})$
$FCL1 = W_{crisp-to-fuzzy}[L11 \cdot D] + b_{crisp-to-fuzzy}$
$V_{crisp} = FCL1_{elements}$
Fuzzification
RETE Network Construction
Values found: $Feature_{value}$, mean, std of V_{crisp}
Memory elements: alpha (α), beta (β)
Rules: rule1=eqn4, rule2=eqn6, rule3=eqn8
Facts: fact1 (eqn5), fact2 (eqn7), fact3 (eqn9)
Nodes: N evolved from V_{crisp}
# Pattern matching
for i in N_{total}, **do**
if N satisfies fact1, attach (rule1 to α(i)), join α(i) to Left β(i-1)
else if N satisfies fact2, attach (rule2 to α(i)), join α(i) to Left β(i-1)
else if N satisfies fact3, attach (rule3 to α(i)), join α(i) to Left β(i-1)
end if
end for
V_{fuzzy}=all values in β
# Defuzzification
for j in β_{total}, **do**
V'_{crisp}= CHI (V_{fuzzy})
end for
$V'_{crisp} = FCL2_{elements}$
$L15$ = softmaxLayer($FCL2$)
for end
Output: Classified result

Algorithm 3 Functions used in pseudo code

function $\mathbf{GRU}_{forward}(x_t)$
$U_t = \sigma(w_u[hf_{t-1}, x_t])$
$R_t = \sigma(w_R[hf_{t-1}, x_t])$
$hf_{intermediate} = tanh(w_h[R_t \cdot hf_{t-1}, x_t])$
$hf_t = (1 - U_t)hf_{t-1} + U_t hf_{intermediate}$
function $\mathbf{GRU}_{backward}(x_t)$
$U_t = \sigma(w_u[hb_{t-1}, x_t])$
$R_t = \sigma(w_R[hb_{t-1}, x_t])$
$hb_{intermediate} = tanh(w_h[R_t \cdot hb_{t-1}, x_t])$
$hb_t = (1 - U_t)hb_{t-1} + U_t hb_{intermediate}$

type 1 fuzzy controller adjusted the weights for the fuzzy membership function based on the backpropagation algorithm. The major reason for implementing the fuzzy logic in the DGFN was to reduce the computational complexity. Generally deep network execution produces a huge number of parameters which becomes difficult to handle. To overcome this drawback fuzzy logic came to the rescue. During the ablation studies, it was observed that the number of parameters and time of network execution got decreased with the presence of fuzzy layers. Finally, DGFN got executed with less than 1 lakh parameters in 3.62 min. While it was seen that without fuzzy layers the parameters were above 1.5 lakh and the time taken for network execution was 5 min approximately.

Different types of activation functions and their corresponding number of hidden layers or units varied for each layer. For BiGRU and GRU layers sigmoid and tanh, respectively, were used as the activation functions. In the case of FF, the activation function RELU was utilized. The number of parameters got generated during the performance curve study, so the values were noted for every network layer. All this information is tabulated in Table 3 in ascending order from the input layer. Evaluation of DGFN over the collected patient data (PPG signals) resulted in an accuracy, recall, precision, sensitivity, specificity, and MAF1-score (Micro-Average F1-score) of 0.85, 0.86, 0.85, 0.86, 0.84,0.85, respectively (Confusion matrix is shown in Fig. 5).

The input dataset was segregated into training and testing sets. Among the training data, there was another split of training and validation. Selection of the best splitting ratio (training: testing) was done by observing the accuracy, recall, precision, specificity, F-score, and FPR as well as the computational cost occurring during the training and evaluation of DGFN. From the stacked bar graph of Fig. 6, it can be seen that when the training and testing split was chosen as 85:15, the highest values of accuracy (0.85), precision(0.86), F-score (0.85), and FPR (0.84) was obtained. Comparatively better accuracy (0.81), recall (0.80), precision(0.82), and FPR (0.80) were found when the data splitting was done in an 80:20 ratio. The results of metrics were low i.e. results were less than 0.80, for the 75:25 and 70:30 splitting ratio.

Proficiency and coherence of DGFN were checked by implementing K-fold cross-validation. The entire experimental data comprising 1740 training and 426 testing samples were randomly shuffled for cross-validating in consecutive folds from 2 to 13. The network was executed and results were derived in terms of performance metric values to find the best K- fold. Minimum results were obtained for the 2-fold validation as shown in the first row of Table 4. There was an increment in results with several folds. Among all the evaluations it was found that 10-fold validation provided the highest result. Thus, the network was cross-validated using 10-fold data. All the evaluation metric values of the network corresponding to each fold are displayed in Table 4. Thus, all suitable measures were examined carefully to prepare the model for best performance (see Table 6).

3.2. Ablation studies

In order to understand the role of each layer, ablation studies were conducted. Initially, we analyzed with the non-fuzzy layers i.e. GRU, Bi-GRU, FF, and MLP layers as shown in Table 5. Gradually, an increment was observed in accuracy, precision, recall, sensitivity, MA F1-score, and specificity by 0.2,0.1,0.3,0.4,0.3, and 0.2, respectively. The three fuzzy membership functions yielded better results than the two fuzzy membership functions (Table 5 and Fig. 8). Comparatively better values of accuracy (0.81), precision (0.79), recall (0.81), sensitivity(0.81), MAF1-score (0.79), and specificity(0.80), were obtained. A steady rise in the above-mentioned parameters was found where recurrent layers and fuzzy layers were added consecutively. Finally, the best results were obtained by arranging appropriate layers as proposed in DGFN (elaborated in Fig. 3). The ROC and PR curves were best presented by the DGFN (Fig. 7a and b). The AUC and AP show the highest values of 0.91 and 0.90, respectively, when DGFN was used. Based on the results of the proposed network over previous combinations of network setup, DGFN was chosen for analyzing the cohort data.

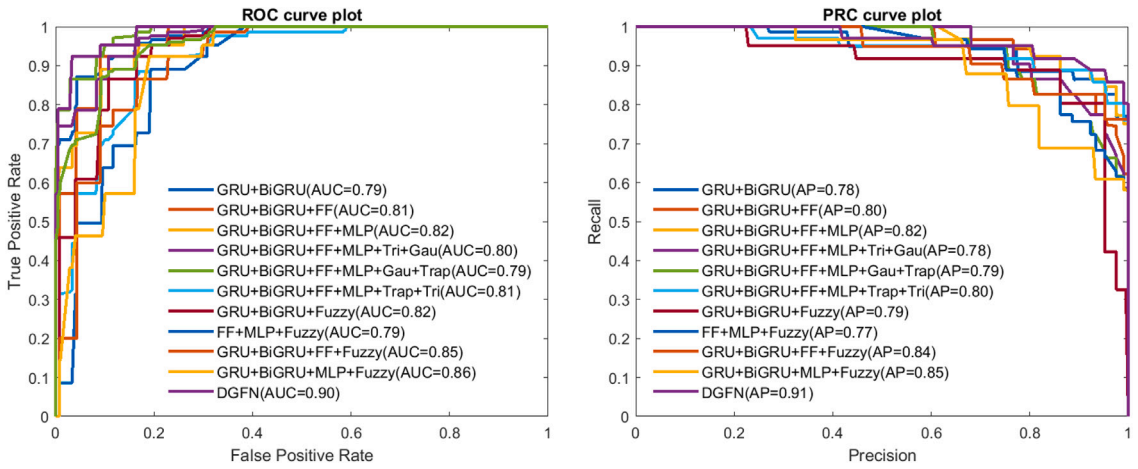

Fig. 7. (a) The ROC curves with AUC values (b) The PR curves with AP values during ablation studies.

Table 5
Result of ablation studies.

Stepwise evolution	Accuracy	Recall	Precision	Sensitivity	Specificity	MAF1-score
GRU+BiGRU	0.78	0.77	0.78	0.76	0.77	0.76
GRU+BiGRU+FF	0.79	0.79	0.77	0.78	0.76	0.78
GRU+BiGRU+FF+MLP	0.80	0.81	0.79	0.80	0.79	0.79
GRU+BiGRU+FF+MLP+Tri+Gau	0.78	0.76	0.75	0.78	0.74	0.77
GRU+BiGRU+FF+MLP+Gau+Trap	0.77	0.78	0.77	0.76	0.75	0.76
GRU+BiGRU+FF+MLP+Tri+Trap	0.79	0.78	0.76	0.79	0.78	0.78
GRU+BiGRU+Fuzzy	0.81	0.81	0.79	0.81	0.80	0.79
FF+MLP+Fuzzy	0.76	0.75	0.74	0.74	0.77	0.75
GRU+BiGRU+FF+Fuzzy	0.82	0.82	0.81	0.83	0.81	0.81
GRU+BiGRU+MLP+Fuzzy	0.82	0.82	0.81	0.83	0.81	0.81
DGFN	0.85	0.86	0.85	0.86	0.84	0.85

Table 6
Performance of various combination of fuzzy membership functions.

Fuzzy layers	Accuracy	Recall	Precision	Sensitivity	Specificity	MAF1-score
Triangular	0.79	0.78	0.78	0.79	0.76	0.76
Gaussian	0.77	0.75	0.76	0.76	0.77	0.75
Trapezoidal	0.78	0.78	0.77	0.76	0.75	0.77
Triangular+Gaussian	0.82	0.81	0.79	0.80	0.80	0.81
Gaussian+Trapezoidal	0.81	0.80	0.82	0.79	0.81	0.80
Trapezoidal+Triangular	0.82	0.81	0.83	0.82	0.81	0.81
Triangular+Gaussian+Trapezoidal	0.84	0.84	0.83	0.83	0.82	0.83

Table 7
Comparison of various standard existing neural network techniques.

+ Fuzzy layer	Accuracy	Recall	Precision	Sensitivity	Specificity	MAF1-s
LSTM	0.76	0.73	0.74	0.72	0.72	0.76
BiLSTM	0.78	0.75	0.76	0.77	0.75	0.76
1D CNN	0.80	0.77	0.78	0.80	0.79	0.80
GRU	0.78	0.77	0.76	0.78	0.77	0.78
BiGRU	0.79	0.78	0.78	0.77	0.79	0.78
GRU+BiGRU	0.81	0.81	0.79	0.81	0.80	0.79

3.3. Comparison with standard classifiers

A comparative study of the DGFN performance was conducted with other standard RNN units (LSTM and BiLSTM) and 1D CNN with fuzzy layers. This helped us to assess the efficacy of the proposed network DGFN. The result of this network was low (<0.8) when LSTM and BiLSTM units were implemented along with fuzzy layers, displayed in Table 7. It was found that the network yielded accuracy = 0.80, recall = 0.77, precision = 0.78, sensitivity = 0.80, specificity = 0.79, and MAF1-score = 0.80 with 1D CNN with fuzzy layers. When GRU + BiGRU with fuzzy layers was used the results were better than the previously mentioned standard techniques (LSTM, BiLSTM, and 1D CNN). The metrics were accuracy = 0.81, recall = 0.81, precision = 0.79, sensitivity = 0.81, specificity = 0.80, and MAF1-score = 0.79. Further comparison was performed using ROC and PR curves (Fig. 9). It can be seen that GRU and BiGRU produced high AUC and AP values. Thus, gated units outperformed the other existing techniques.

3.4. State-of-the-art

Various studies involving the analysis of PPG signals from IHD patients were carried out with different techniques. These works along with the number of subjects involved in the study, the methodology used, and their results are elaborated on in Table 8. Signal analysis by feature extraction and application of machine learning and deep learning (DL)classifiers were conducted by Banerjee et al. [12], Hosseini et al. [13], Shiyovich et al. [15], Banerjee et al. [32], Anirban et al. [35], Sadaf et al. [33], and Jaehak et al. [34]. Specifically, SVM, KNN, and logistic regression (LR) were used as the classification tool on subjects less than 200 to produce results around accuracy = 0.80. Neural networks were implemented by Fathieh et al. [14] and Silveri et al. [31]. Elastic net on 408 subjects and ANN on 965 subjects

Table 8
Study of the state of the art methods.

Past works	Year	Patients	Method	Accuracy	Sensitivity	Specificity	AUC
Banerjee et al. [12]	2018	99	SVM	–	0.80	0.80	–
Hosseini et al. [13]	2015	48	KNN	0.81	0.82	0.80	–
Fathieh et al. [14]	2021	408	EN	–	0.80	0.80	0.90
Shiyovich et al. [15]	2010	193	LR	–	0.83	0.70	–
Silveri et al. [31]	2020	965	ANN	0.82	–	–	–
Banerjee et al. [32]	2017	25	SVM	0.80	0.60	0.93	–
Sadaf et al. [33]	2023	37	DL	0.80	–	–	–
Jaehak et al. [34]	2022	287	CNN+LSTM	0.96	–	–	–
Anirban et al. [35]	2018	32	GNN	0.88	–	–	–
Proposed work	2023	1550	DGFN	0.85	0.86	0.84	0.91
	Year	PPG signals	Method	Accuracy	Sensitivity	Specificity	AUC
|	2018	99	SVM	0.79	0.80	0.80	0.81
|	2015	48	KNN	0.78	0.79	0.77	0.78
|	2021	408	EN	0.82	0.83	0.82	0.85
|	2010	193	LR	0.80	0.82	0.81	0.82
Results on collected data	2020	965	ANN	0.83	0.82	0.81	0.82
|	2017	25	SVM	0.72	0.65	0.63	0.70
|	2023	37	DL	0.82	0.81	0.82	0.84
|	2022	287	CNN+LSTM	0.81	0.83	0.83	0.85
|	2018	32	GNN	0.83	0.81	0.82	0.87
|	2023	1550	DGFN	0.85	0.86	0.84	0.91

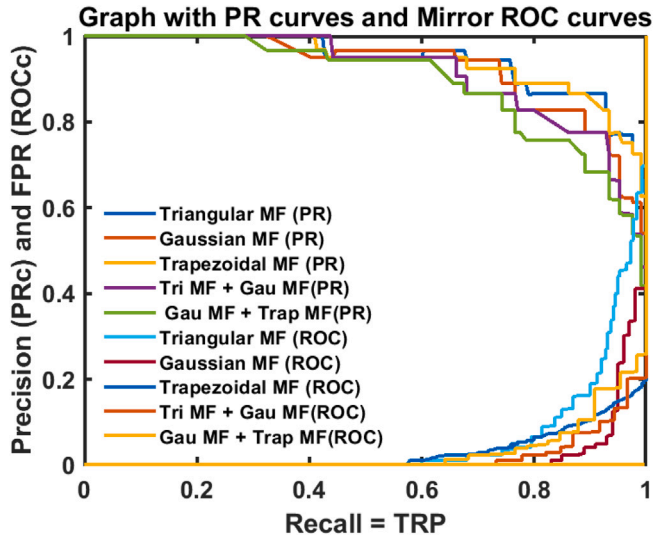

Fig. 8. Combined plot with PR curves and mirror ROC curves for comparing performance of fuzzy membership functions.

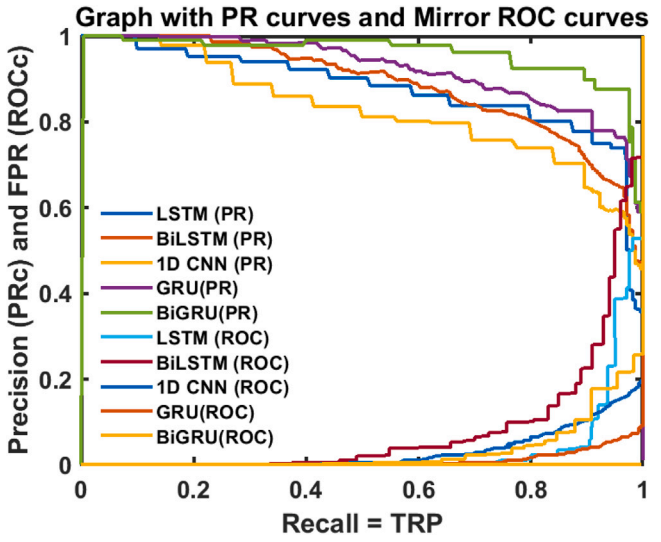

Fig. 9. Merged mirror ROC curve (ROCc) and PR curve (PRc) to compare the performance of DGFN with existing standard techniques.

produced better results. The introduction of fuzzy concepts amidst neural network layers produced the highest result. Sadaf et al. [33], Jaehak et al. [34], and Anirban et al. [35] used DL, CNN+LSTM, and graph neural network (GNN) on 37,287, and 32 patients to classify signals with accuracy of 0.80, 0.96, and 0.88, respectively. When DGFN was executed on the 1550 signals, accuracy of 0.85, sensitivity of 0.86, specificity of 0.84, and AUC of 0.91 was obtained. For uniform comparison, techniques of [12–32] were implemented on our collected PPG signals, same hyperparameters, and computational environment. Classification performance metrics and AUC were < 0.85, 0.86, 0.84, and 0.91 with their methods (Table 8). The classification results of DGFN showed the superiority of this proposed model over the state-of-the-art methods in analyzing PPG signals from patients.

4. Discussions

The results of this study exhibit that the proposed DGFN can classify IHD patients based on treatment suggested by cardiologists. Further, an advantage of this experimental study is its simplicity in collecting data, feasibility, portability, and quick results. The inclusion of fuzzy logic in GRU network surpassed the results given by other techniques. The preliminary results of this cohort study show that this diagnosing model could become a foundation in clinical decision support system for deciding treatment of IHD patients in the future.

For further validation, DGFN was also executed on two PPG-based databases [36,37]. Though these PPG signals were not analyzed for IHD patients, still to observe the classification ability of DGFN, proposed network was executed on these online data sets. The classification results from BUT PPG and MIMIC-III Waveform Database gave accuracy, recall, precision, sensitivity, specificity, MAF1-score of 83%, 82%, 83%, 81%, 80%, 82%, and 75%, 77%, 78%, 79%, 74%, 76%, respectively. These results were superior to the results mentioned in previous literature.

In the future DGFN can be made more versatile and dynamic by including co-morbid patient data. this model can further be modified to execute on patients with different diseases for broadening its spectrum.

5. Conclusion

This study demonstrates how non-invasive PPG signals can be used to predict the type of therapy for IHD patients. This technique is inexpensive, portable, and might provide a fast mode of IHD diagnosis. The application of Fuzzy layers embedded within the GRU layers has never been reported to the best of the authors' knowledge. Here, the fuzzy membership functions are incorporated to enhance the network feature values for classification purposes. The concept Rete network was used for fuzzification. Defuzzification was performed using Choquet Integral. However, the proposed model needs to become more robust, for which the validation has to be carried out on new patient data at a large scale. The co-morbid IHD patient data were excluded from the input database, this limited the flexibility of the classification model. Encouraging results of 0.85-accuracy, 0.86-recall, 0.85-precision, 0.86-sensitivity, 0.85-MAF1-score, and 0.84-specificity, inspired the idea that PPG signals could be introduced in the clinical field for instant and low-cost assessment of IHD patients using DGFN. In the future, this model could be evolved as a point-of-care technique for ischemic patients.

CRediT authorship contribution statement

Poulomi Pal: Conception and design of study, Acquisition of data, Analysis and/or interpretation of data, Writing – original draft, Writing – review & editing. **Manjunatha Mahadevappa:** Conception and design of study, Acquisition of data, Analysis and/or interpretation of data, Writing – original draft, Writing – review & editing.

Declaration of competing interest

The authors declare that they have no known competing financial interests or personal relationships that could have appeared to influence the work reported in this paper.

Data availability

The authors do not have permission to share data

Acknowledgments

The authors acknowledge Dr. Bhawani Prasad Chattopadhyay, associate professor and cardiologist, medical college and hospital, kolkata, for clinical support, cohort patients, and medical staff of hospital. Authors thank Dr. Kapudeep Karmakar, associate professor from Uttar Banga Krishi Vishwavidyalaya, West Bengal, for proof-reading the manuscript. All authors approved the version of the manuscript to be published.

Funding

This research did not receive any specific grant from funding agencies in the public, commercial, or not-for-profit sectors.

Ethical approval

The Institutional Ethical Clearance vide reference number: MC/Kol/IEC/Non-spon/139/09- 2018 dated 10-11-2018 from Medical College and Hospital Kolkata and IIT/ SRIC/DR/2019, dated 6-11-2019 from Indian Institute of Technology Kharagpur.

References

[1] H. Dai, A.A. Much, E. Maor, E. Asher, A. Younis, Y. Xu, Y. Lu, X. Liu, J. Shu, N.L. Bragazzi, Global, regional, and national burden of ischaemic heart disease and its attributable risk factors, 1990–2017: results from the global burden of disease study 2017, Eur. Heart J.-Qual. Care Clin. Outcomes 8 (1) (2022) 50–60.

[2] M.A. Khan, M.J. Hashim, H. Mustafa, M.Y. Baniyas, S.K.B.M. Al Suwaidi, R. AlKatheeri, F.M.K. Alblooshi, M.E.A.H. Almatrooshi, M.E.H. Alzaabi, R.S. Al Darmaki, et al., Global epidemiology of ischemic heart disease: results from the global burden of disease study, Cureus 12 (7) (2020).

[3] M.U. Khan, S. Aziz, K. Iqtidar, R. Fernandez-Rojas, Computer-aided diagnosis system for cardiac disorders using variational mode decomposition and novel cepstral quinary patterns, Biomed. Signal Process. Control 81 (2023) 104509.

[4] A. Rath, D. Mishra, G. Panda, S.C. Satapathy, Heart disease detection using deep learning methods from imbalanced ECG samples, Biomed. Signal Process. Control 68 (2021) 102820.

[5] M. Tavakol, S. Ashraf, S.J. Brener, Risks and complications of coronary angiography: a comprehensive review, Glob. J. Health Sci. 4 (1) (2012) 65.

[6] P.T. Kariyanna, L. Aurora, A. Jayarangaiah, S. Das, J.C. Gonzalez, S. Hegde, I.M. McFarlane, Neurotoxicity associated with radiological contrast agents used during coronary angiography: a systematic review, Am. J. Med. Case Rep. 8 (2) (2020) 60.

[7] J.W. Kennedy, W.A. Baxley, I.L. Bunnel, G.G. Gensini, J.V. Messer, J.G. Mudd, T.J. Noto, S. Paulin, A.D. Pichard, W.C. Sheldon, et al., Mortality related to cardiac catheterization and angiography, Cathet. Cardiovasc. Diagn. 8 (4) (1982) 323–340.

[8] A.R. Kavsaoğlu, K. Polat, M. Hariharan, Non-invasive prediction of hemoglobin level using machine learning techniques with the PPG signal's characteristics features, Appl. Soft Comput. 37 (2015) 983–991.

[9] A. Baccouche, B. Garcia-Zapirain, C. Castillo Olea, A. Elmaghraby, Ensemble deep learning models for heart disease classification: A case study from Mexico, Information 11 (4) (2020) 207.

[10] K. Dubey, A. Agarwal, A.S. Lathe, R. Kumar, V. Srivastava, Self-attention based BiLSTM-CNN classifier for the prediction of ischemic and non-ischemic cardiomyopathy, 2019, arXiv preprint arXiv:1907.10370.

[11] P. Pal, S. Ghosh, B.P. Chattopadhyay, K.K. Saha, M. Mahadevappa, Screening of ischemic heart disease based on PPG signals using machine learning techniques, in: 2020 42nd Annual International Conference of the IEEE Engineering in Medicine & Biology Society (EMBC), IEEE, 2020, pp. 5980–5983.

[12] R. Banerjee, S. Bhattacharya, S. Alam, Time series and morphological feature extraction for classifying coronary artery disease from photoplethysmogram, in: 2018 IEEE International Conference on Acoustics, Speech and Signal Processing (ICASSP), IEEE, 2018, pp. 950–954.

[13] Z.S. Hosseini, E. Zahedi, H.M. Attar, H. Fakhrzadeh, M.H. Parsafar, Discrimination between different degrees of coronary artery disease using time-domain features of the finger photoplethysmogram in response to reactive hyperemia, Biomed. Signal Process. Control 18 (2015) 282–292.

[14] F. Fathieh, M. Paak, A. Khosousi, T. Burton, W.E. Sanders, A. Doomra, E. Lange, R. Khedraki, S. Bhavnani, S. Ramchandani, Predicting cardiac disease from interactions of simultaneously-acquired hemodynamic and cardiac signals, Comput. Methods Programs Biomed. 202 (2021) 105970.

[15] A. Shiyovich, J. Jafari, Y. Blaer, H. Rehby, I. Orlov, D. Cohen, A. Katz, Respiratory stress response: a novel diagnostic method for detection of significant coronary artery disease from finger pulse wave analysis during brief respiratory exercise, Am. J. Med. Sci. 339 (5) (2010) 440–447.

[16] A. Dourado, J. Henriques, P.d. Carvalho, Neural, fuzzy, and neurofuzzy systems for medical applications, Intell. Adapt. Syst. Med. (2008) 127–171.

[17] A. Farahabadi, E. Farahabadi, H. Rabbani, M.P. Mahjoub, A.M. Dehnavi, Ischemia detection via dynamic time warping and fuzzy rules, in: Proceedings of 2012 IEEE-EMBS International Conference on Biomedical and Health Informatics, IEEE, 2012, pp. 166–169.

[18] J. Rivera, K. Rodriguez, X.-H. Yu, Cardiovascular conditions classification using adaptive neuro-fuzzy inference system, in: 2019 IEEE International Conference on Fuzzy Systems (FUZZ-IEEE), IEEE, 2019, pp. 1–6.

[19] D. Gabor, Theory of communication. Part 1: The analysis of information, J. Inst. Electr. Eng.-Part III: Radio Commun. Eng. 93 (26) (1946) 429–441.

[20] K. Cho, B. Van Merriënboer, D. Bahdanau, Y. Bengio, On the properties of neural machine translation: Encoder-decoder approaches, 2014, arXiv preprint arXiv:1409.1259.

[21] S.R. Price, S.R. Price, D.T. Anderson, Introducing fuzzy layers for deep learning, in: 2019 IEEE International Conference on Fuzzy Systems (FUZZ-IEEE), IEEE, 2019, pp. 1–6.

[22] J. Wu, R. Hu, M. Li, S. Liu, X. Zhang, J. He, J. Chen, X. Li, Diagnosis of sleep disorders in traditional Chinese medicine based on adaptive neuro-fuzzy inference system, Biomed. Signal Process. Control 70 (2021) 102942.

[23] D. Bonanno, K. Nock, L. Smith, P. Elmore, F. Petry, An approach to explainable deep learning using fuzzy inference, in: Next-Generation Analyst V, Vol. 10207, International Society for Optics and Photonics, 2017, 102070D.

[24] M.H. Vafaie, M. Ataei, H.R. Koofigar, Heart diseases prediction based on ECG signals' classification using a genetic-fuzzy system and dynamical model of ECG signals, Biomed. Signal Process. Control 14 (2014) 291–296.
[25] T. Nguyen, A. Khosravi, D. Creighton, S. Nahavandi, Fuzzy system with tabu search learning for classification of motor imagery data, Biomed. Signal Process. Control 20 (2015) 61–70.
[26] M. Lee, T.-G. Song, J.-H. Lee, Heartbeat classification using local transform pattern feature and hybrid neural fuzzy-logic system based on self-organizing map, Biomed. Signal Process. Control 57 (2020) 101690.
[27] P. Angelov, X. Zhou, D. Filev, E. Lughofer, Architectures for evolving fuzzy rule-based classifiers, in: 2007 IEEE International Conference on Systems, Man and Cybernetics, IEEE, 2007, pp. 2050–2055.
[28] C.L. Forgy, Rete: A fast algorithm for the many pattern/many object pattern match problem, in: Readings in Artificial Intelligence and Databases, Elsevier, 1989, pp. 547–559.
[29] V. Torra, J. Garcia-Alfaro, Towards an adaptive defuzzification: using numerical choquet integral, in: International Conference on Modeling Decisions for Artificial Intelligence, Springer, 2019, pp. 113–125.
[30] D. Połap, Automatic fuzzy parameter tuning for neural network models, in: 2022 IEEE International Conference on Fuzzy Systems (FUZZ-IEEE), IEEE, 2022, pp. 1–5.
[31] G. Silveri, M. Merlo, L. Restivo, G. Sinagra, A. Accardo, Novel classification of ischemic heart disease using artificial neural network, in: 2020 Computing in Cardiology, IEEE, 2020, pp. 1–4.
[32] R. Banerjee, A.D. Choudhury, S. Datta, A. Pal, K.M. Mandana, Non invasive detection of coronary artery disease using pcg and ppg, in: EHealth 360°, Springer, 2017, pp. 241–252.
[33] S. Iqbal, S. Agarwal, I. Purcell, A. Murray, J. Bacardit, J. Allen, Deep learning identification of coronary artery disease from bilateral finger photoplethysmography sensing: A proof-of-concept study, Biomed. Signal Process. Control 86 (2023) 104993.
[34] J. Yu, S. Park, S.-H. Kwon, K.-H. Cho, H. Lee, AI-based stroke disease prediction system using ECG and ppg bio-signals, IEEE Access 10 (2022) 43623–43638.
[35] A.D. Choudhury, A.S. Chowdhury, Change: Cardiac health analysis using graph eigenvalues, in: 2018 40th Annual International Conference of the IEEE Engineering in Medicine and Biology Society (EMBC), IEEE, 2018, pp. 4025–4029.
[36] A. Nemcova, R. Smisek, E. Vargova, L. Maršánová, M. Vitek, L. Smital, Brno university of technology smartphone PPG database (BUT PPG), PhysioNet (2021).
[37] B. Moody, G. Moody, M. Villarroel, G. Clifford, I. Silva, MIMIC-III waveform database matched subset (version1. 0). PhysioNet, 2020.